Syntheses, Structures, and Properties of $[Mn_2(\mu\text{-}O)_2(\mu\text{-}O_2CCH_3)(fac\text{-}bpea)_2](ClO_4)_2$ and Two Halide-Ligated Dioxo-Bridged Dimers Derived Therefrom: $[Mn_2(\mu\text{-}O)_2X_2(mer\text{-}bpea)_2](ClO_4)_2$ (X = F, Cl)[1]

Samudranil Pal,[†] Marilyn M. Olmstead,[‡] and William H. Armstrong*[,§]

Department of Chemistry, University of California, Berkeley, California 94720, Department of Chemistry, University of California, Davis, California 95616, and Department of Chemistry, Eugene F. Merkert Chemistry Center, Boston College, Chestnut Hill, Massachusetts 02167-3860

Received January 6, 1993[⊗]

The reaction of $Mn(O_2CCH_3)_2{\cdot}4H_2O$, *N,N*-bis(2-pyridylmethyl)ethylamine (bpea), and $KMnO_4$ in aqueous acetate buffer (pH ~4.5) afforded the mixed-valence complex $[Mn_2O_2(O_2CCH_3)(bpea)_2](ClO_4)_2$ (**1**) in 79% yield. Diffusion of *n*-hexane into a solution of **1** in CH_2Cl_2 provided the CH_2Cl_2 disolvate, which crystallizes in space group $P\bar{1}$ with $a = 9.293(2)$ Å, $b = 12.233(2)$ Å, $c = 18.812(3)$ Å, $\alpha = 92.781(13)°$, $\beta = 99.636(19)°$, $\gamma = 97.727(16)°$, $V = 2083.6(15)$ Å^3, and $Z = 2$. Compound **1** is an example of a trapped mixed-valence $Mn^{III}Mn^{IV}$ species for which the Mn(III) and Mn(IV) ions are easily distinguishable in the solid state. The electronic and EPR spectral properties of **1** in CH_3CN are characteristic of the $\{Mn_2O_2\}^{3+}$ core. The cyclic voltammogram of **1** in CH_3CN shows III,IV to IV,IV oxidation and III,IV to III,III reduction waves at +0.92 and +0.02 V, respectively, vs SCE. Variable-temperature magnetic susceptibility measurements of **1** in the solid state confirmed a doublet ground state. These magnetic data have been fitted adequately using the isotropic spin Hamiltonian $\mathcal{H} = -2JS_1{\cdot}S_2$ ($S_1 = 2$, $S_2 = {}^3/_2$) with $J = -164$ cm^{-1}. Compound **1** was converted to $[Mn_2O_2X_2(bpea)_2](ClO_4)_2$ (X = F, **2**; X = Cl, **3**) by addition of 2 equiv of aqueous HX in CH_3CN. Formation of the halide derivatives is presumed to be the result of a disproportionation reaction. Crystal structure determinations of **2** and **3** were performed. Both species crystallize in the space group $P\bar{1}$ on crystallographic inversion centers. The unit cell parameters for **2** are $a = 6.692(2)$ Å, $b = 10.751(3)$ Å, $c = 12.179(2)$ Å, $\alpha = 69.07(2)°$, $\beta = 79.25(2)°$, $\gamma = 81.46(3)°$, $V = 801.3(4)$ Å^3, and $Z = 1$ and for **3** are $a = 7.187(2)$ Å, $b = 10.669(3)$ Å, $c = 12.531(3)$ Å, $\alpha = 113.72(2)°$, $\beta = 99.73(2)°$, $\gamma = 94.32(2)°$, $V = 856.0(4)$ Å^3, and $Z = 1$. Bond distances to Mn ions in **2** and **3** are consistent with these ions being in the +4 formal oxidation state. Compounds **2** and **3** have two prominent electronic absorption bands in the visible region: **2**, 530, 635 nm; **3**, 550, 642 nm. Assignment of similar bands in III,IV binuclear species appears elsewhere (*J. Am. Chem. Soc.* **1994**, *116*, 2392). Less intense low-energy maxima in the vicinity of 800 nm were observed for both compounds as well. Cyclic voltammetry experiments conducted in CH_3CN revealed two reduction responses for both **2** and **3**. They are assigned as IV,IV to III,IV and III,IV to III,III reductions. The potentials (vs SCE) for these processes are +0.59 and −0.35 V, respectively, for **2** and +0.74 and −0.06 V, respectively, for **3**. Variable-temperature magnetic susceptibility measurements reveal the presence of an antiferromagnetic interaction between the two Mn(IV) centers in complex **3**. The magnitude of the coupling constant *J*, obtained by least-squares fitting of the magnetic susceptibility data for **3** using an expression generated from the isotropic spin Hamiltonian $\mathcal{H} = -2JS_1{\cdot}S_2$ ($S_1 = {}^3/_2$, $S_2 = {}^3/_2$), is −147 cm^{-1}. The infrared absorption spectra for compounds **1**−**3** were measured.

Introduction

The active site for water oxidation in photosystem II is thought to be an oxo-bridged polynuclear manganese complex,[2] referred to herein as MnPSII, within which there are probably at least two 2.7 Å Mn···Mn contacts. Evidence for these relatively short Mn···Mn distances comes from X-ray absorption spectral measurements.[3] Electron paramagnetic resonance (EPR) spectroscopy is also commonly employed to probe MnPSII.[4] Despite a growing body of data from the aforementioned and other physical characterization techniques, there remains no consensus with regard to the precise three-dimensional structure of the manganese aggregate. The existence of this important polynuclear oxo-bridged aggregate in Nature has prompted a great deal of activity among synthetic inorganic chemists directed toward the preparation of a small molecule analog.[2,5,6] While a variety of interesting species, including many binuclear dioxo-bridged complexes, have been

[†] Current address: School of Chemistry, University of Hyderabad, Central University P.O., Hyderabad 500 134, India.

[‡] University of California, Davis.

[§] Current address: Department of Chemistry, Eugene F. Merkert Chemistry Center, Boston College, Chestnut Hill, MA 02167-3860.

[⊗] Abstract published in *Advance ACS Abstracts,* August 1, 1995.

(1) Abbreviations used: PS II, photosystem II; EPR, electron paramagnetic resonance; IR, infrared; SCE, saturated calomel electrode; TEAP, tetraethylammonium perchlorate; bpea, *N,N*-bis(2-pyridylmethyl)-ethylamine; tpen, *N,N,N′,N′*-tetrakis(2-pyridylmethyl)-1,2-ethanediamine; bpy, 2,2′-bipyridine; tacn, 1,4,7-triazacyclononane; cyclam, 1,4,8,11-tetraazacyclotetradecane; *fac*, facial; *mer*, meridional.

(2) (a) Debus, R. J. *Biochim. Biophys. Acta* **1992**, *1102*, 269−352. (b) Armstrong, W. H. In *Manganese Redox Enzymes*; Pecoraro, V. L., Ed.; VCH: New York, 1992; pp 261−286. (c) Pecoraro, V. L. *Ibid.*, pp 197−231. (d) Wieghardt, K. *Angew. Chem., Int. Ed. Engl.* **1989**, *28*, 1153−1172. (e) Brudvig, G. W.; Crabtree, R. H. *Prog. Inorg. Chem.* **1989**, *37*, 99−142. (f) Babcock, G. T. In *New Comprehensive Biochemistry: Photosynthesis*; Amesz, J., Ed.; Elsevier: Amsterdam, 1987; pp 125−158. (g) Que, L., Jr.; True, A. E. *Prog. Inorg. Chem.* **1990**, *38*, 97−200.

(3) (a) DeRose, V. J.; Mukerji, I.; Latimer, M. J.; Yachandra, V. K.; Sauer, K.; Klein, M. P. *J. Am. Chem. Soc.* **1994**, *116*, 5239−5249. (b) Yachandra, V. K.; Guiles, R. D.; McDermott, A. E.; Cole, J. L.; Britt, R. D.; Dexheimer, S. L.; Sauer, K.; Klein, M. P. *Biochemistry* **1987**, *26*, 5974−5981. (c) George, G. N.; Prince, R. C.; Cramer, S. P. *Science* **1989**, *243*, 789−791. (d) Penner-Hahn, J. E.; Fronko, R. M.; Pecoraro, V. L.; Yocum, C. F.; Betts, S. D.; Bowlby, N. R. *J. Am. Chem. Soc.* **1990**, *112*, 2549−2557.

0020-1669/95/1334-4708$09.00/0

reported, an exact replica of the enzyme catalytic site manganese aggregate has not been realized.

A portion of our efforts in this research area have been devoted to the development of the coordination chemistry of oxo-bridged manganese aggregates employing the tridentate ligand bpea (*N,N*-bis(2-pyridylmethyl)ethylamine). Recently we reported[5] a preparation of the dimanganese(IV) species $[Mn_2O_2(O_2CCH_3)(bpea)_2]^{3+}$ and noted that it was unstable in aqueous solution with respect to formation of a trinuclear complex, $[Mn_3O_4(OH)(bpea)_3]^{3+}$. While this latter species displays fascinating electronic properties, we are interested in a controlled aggregation process involving the coupling of two binuclear species leading to formation of a tetranuclear end product. A great deal of emphasis in the MnPSII modeling field has been placed on tetranuclear structural types[6] as there is evidence that four manganese atoms per water oxidation enzyme are required for optimal activity. The first step in one approach to controlled aggregation involves removal of the bridging acetate group from a species containing the $\{Mn_2O_2(O_2CCH_3)\}$ core, replacing it with monodentate ligands such as halide. Herein we demonstrate that the one-electron-reduced derivative of the dimanganese(IV) compound mentioned above, namely $[Mn_2O_2(O_2CCH_3)(bpea)_2]^{2+}$ (**1**), can be converted to acetate-free dihalide dimers, $[Mn_2O_2X_2(bpea)_2]^{2+}$ (X = F, **2**; X = Cl, **3**) by addition of the appropriate hydrohalous acid. Structurally uncharacterized species similar to **2** and **3**, yet presumably having different geometries due to the rigid facial coordination mode associated with the ligand 1,4,7-triazacyclononane (tacn), have been prepared by Weighardt and coworkers.[7]

The flexibility of the bpea ligand with respect to adopting either a facial or a meridional coordination mode is highlighted here for the first time. Also, as chloride is required for efficient photochemically driven water oxidation by MnPSII, it is important to prepare novel small molecules bearing chloride ligands so that the effect of these donors on the physical and chemical properties of manganese–oxo aggregates can be examined. Finally, while fluoride is not required for MnPSII activity but rather inhibits it, this anion has a dramatic effect on the EPR spectral properties of MnPSII in the Kok S_2 state.[8] An understanding of this phenomenon may come eventually from examination of fluoride-ligated manganese clusters.

Experimental Section

Materials. The ligand *N,N*-bis(2-pyridylmethyl)ethylamine (bpea) was prepared as described previously.[5] For electrochemical experiments, acetonitrile was distilled from CaH_2 and stored over 3 Å molecular sieves prior to use. The supporting electrolyte tetraethylammonium perchlorate (TEAP) was prepared by following a reported procedure.[9] All other solvents and chemicals used in this work were of analytical grade and were used as supplied.

Physical Measurements. IR spectra were recorded for KBr pellets of **1**–**3** by using a Nicolet 5DX Fourier transform infrared spectrometer. A Varian Cary 2400 UV–vis–near-IR or a Perkin-Elmer Lambda 3B UV–vis spectrophotometer was used to collect the electronic spectra. The X-band EPR spectrum was recorded at liquid nitrogen temperature using an immersion "finger" dewar in an IBM 2090D-SRC spectrometer. Solid state magnetic susceptibility measurements were performed at Tufts University with use of a Quantum Design Model MPMS SQUID magnetometer operating in the temperature range 6–280 K at a constant applied magnetic field of 5 kG. All data were corrected for the susceptibility of the empty sample container. Molar paramagnetic susceptibilities were obtained by using diamagnetic corrections (-442×10^{-6} and -462×10^{-6} cgsu for **1** and **3**, respectively) calculated from Pascal's constants.[10] Cyclic voltammetry experiments were done with an EG&G PAR Model 273 potentiostate/galvanostat equipped with a PAR Model RE 0091 X-Y recorder. A standard three-electrode cell consisting of a platinum disk working electrode, a platinum wire auxiliary electrode, and a saturated calomel reference electrode (SCE) was used to collect the cyclic voltammograms. All electrochemical measurements were performed under a dry, purified dinitrogen or argon atmosphere. The potentials reported in this work are uncorrected for junction contributions. Using the conditions described above, the ferrocene/ferrocenium redox couple was observed at 0.39 V vs SCE. Elemental analyses were obtained from the University of California, Berkeley Microanalytical Laboratory.

CAUTION: While we have not experience problems with the compounds listed below, perchlorate salts of compounds containing organic ligands are potentially explosive![11]

Preparation of Compounds. $[Mn_2O_2(O_2CCH_3)(bpea)_2](ClO_4)_2$ (1). To a methanol solution (10 mL) of bpea (1.42 g, 6.25 mmol) were added with stirring solid $Mn(O_2CCH_3)_2{\cdot}4H_2O$ (1.07 g, 4.37 mmoll) and 25 mL of acetate buffer (pH = 4.5). The clear solution was cooled to approximately 0 °C, and an aqueous solution (15 mL) of $KMnO_4$ (296 mg, 1.87 mmol) was added slowly with continuous stirring. The resulting dark green-brown solution was stirred for 15 min. The green precipitate formed by the addition of an aqueous solution (5 mL) of 2 g (0.014 mol) of $NaClO_4{\cdot}H_2O$ was collected by filtration and air-dried. The resulting solid was extracted with CH_2Cl_2. The green-brown

(4) (a) Hansson, O.; Andréasson, L. E. *Biochim. Biophys. Acta* **1982**, *679*, 261–268. (b) Dismukes, G. C.; Siderer, Y. *Proc. Natl. Acad. Sci. U.S.A.* **1981**, *78*, 274–278. (c) Zimmermann, J. L.; Rutherford, A. W. *Biochemistry* **1986**, *25*, 4609–4615. (d) Miller, A.-F.; Brudvig, G. W. *Biochim. Biophys. Acta* **1991**, *1056*, 1–18. (e) Kim, D. H.; Britt, R. D.; Klein, M. P.; Sauer, K. *J. Am. Chem. Soc.* **1990**, *112*, 9389–9391. (f) Dexheimer, S. L.; Sauer, K.; Klein, M. P. In *Current Research in Photosynthesis*; Battscheffsky, M., Ed.; Kluwer Academic Publishers: Dordrecth, The Netherlands, 1990; Vol. 1, pp 761–764. (g) Dexheimer, S. L.; Klein, M. P. *J. Am. Chem. Soc.* **1992**, *114*, 2821–2826.

(5) Pal, S.; Chan, M. K.; Armstrong, W. H. *J. Am. Chem. Soc.* **1992**, *114*, 6398–6406.

(6) (a) Wieghardt, K.; Bossek, U.; Gebert, W. *Angew. Chem., Int. Ed. Engl.* **1983**, *22*, 328–329. (b) Bashkin, J. S.; Chang, H. R.; Streib, W. E.; Huffman, J. C.; Christou, G.; Hendrickson, D. N. *J. Am. Chem. Soc.* **1987**, *109*, 6502–6504. (c) Kulawiec, R. J.; Crabtree, R. H.; Brudvig, G. W.; Schulte, G. K. *Inorg. Chem.* **1988**, *27*, 1309–1311. (d) Li, Q.; Vincent, J. B.; Chang, H.-R.; Huffman, J. C.; Boyd, P. D. W.; Christou, G.; Hendrickson, D. N. *Angew. Chem., Int. Ed. Engl.* **1988**, *27*, 1731–1733. (e) Hagen, K. S.; Westmoreland, T. D.; Scott, M. J.; Armstrong, W. H. *J. Am. Chem. Soc.* **1989**, *111*, 1907–1909. (f) Vincent, J. B.; Christmas, C.; Chang, H.-R.; Li, Q.; Boyd, P. D. W.; Huffman, J. C.; Hendrickson, D. N.; Christou, G. *J. Am. Chem. Soc.* **1989**, *111*, 2086–2097. (g) Chan, M. K.; Armstrong, W. H. *J. Am. Chem. Soc.* **1989**, *111*, 9121–99122. (h) Suzuki, M.; Sugisawa, T.; Senda, H.; Oshio, H.; Uehara, A. *Chem. Lett.* **1989**, 1091–1094. (i) Chan, M. K.; Armstrong, W. H. *J. Am. Chem. Soc.* **1990**, *112*, 4985–4986. (j) Suzuki, M.; Senda, H.; Suenaga, M.; Sugisawa, T.; Uehara, T. *Chem. Lett.* **1990**, 923–926. (k) Stibrany, R. T.; Gorun, S. M. *Angew. Chem., Int. Ed. Engl.* **1990**, *29*, 1156–1158. (l) Chan, M. K.; Armstrong, W. H. *J. Am. Chem. Soc.* **1991**, *113*, 5055–5057. (m) Chandra, S. K.; Chakravorty, A. *Inorg. Chem.* **1991**, *30*, 3795–3796. (n) Suzuki, M.; Hayashi, Y.; Munezawa, K.; Suenaga, M.; Senda, H.; Uehara, A. *Chem. Lett.* **1991**, 1929–1932. (o) Bouwman, E.; Bolcar, M. A.; Libby, E.; Huffman, J. C.; Folting, K.; Christou, G. *Inorg. Chem.* **1992**, *31*, 5185–5192. (p) Mikuriya, M.; Yamato, Y.; Tokki, T. *Bull. Chem. Soc. Jpn.* **1992**, *65*, 2624–2637.

(7) Wieghardt, K.; Bossek, U.; Zsolani, L.; Huttner, G.; Blondin, G.; Girerd, J.-J.; Babonneau, F. *J. Chem. Soc., Chem. Commun.* **1987**, 651–653.

(8) (a) Casey, J. L.; Sauer, K. *Biochim. Biophys. Acta* **1984**, *767*, 21–28. (b) Beck, W. F.; Brudvig, G. W. *Chem. Scr.* **1988**, *28A*, 93–98. (c) Ono, T.-A.; Nakayama, H.; Gleiter, H.; Inoue, Y.; Kawamori, A. *Arch. Biochem. Biophys.* **1987**, *256*, 618–624. (d) Yachandra, V. K.; Guiles, R. D.; Sauer, K.; Klein, M. P. *Biochim. Biophys. Acta* **1986**, *850*, 333–342. (e) DeRose, V. J. Ph.D. Dissertation, University of California; Lawrence Berkeley Laboratory Report No. LBL-30077, 1990; Chapter 4.

(9) Sawyer, D. T.; Roberts, J. L. In *Experimental Electrochemistry for Chemists*; Wiley: New York, 1974; p 212.

(10) Hatfield, W. E. In *Theory and Applications of Molecular Paramagnetism*; Boudreaux, E. A., Mulay, L. N., Eds.; Wiley: New York, 1976; pp 491–495.

(11) Wolsey, W. C. *J. Chem. Educ.* **1973**, *50*, A335–A337.

dichloromethane extract was filtered, and the filtrate was evaporated to dryness by using a rotary evaporator. The yield of the dark solid obtained in this manner was 2.12 g (79%). This material was found to be of suitable purity for use as a starting material in the reactions described below. Anal. Calcd for $Mn_2C_{30}H_{37}N_6Cl_2O_{12}$: Mn, 12.86; C, 42.17; H, 4.36; N, 9.84. Found: Mn, 12.6; C, 42.41; H, 4.35; N, 9.25. Prominent IR bands[12] (cm^{-1}): 1610(s), 1574(m), 1563(s), 1486(s), 1437(s), 1387(s), 1337(s), 1308(w), 1290(m), 1161(m), 1094(vs), 1056(sh), 1032(m), 997(w), 769(s), 731(w), 719(w), 693(s), 681(sh), 669(sh), 660(m), 622(s), 608(m), 549(w), 430(m). Electronic spectral data[12] in CH_3CN (λ, nm (ϵ, M^{-1} cm^{-1})): 633(350), 545(420), 490(sh), 455(sh), 390(sh).

$[Mn_2O_2F_2(bpea)_2](ClO_4)_2$ (2). A 48% aqueous HF solution (0.1 mL, 2.76 mmol) was diluted to a volume of 10 mL with acetonitrile. A 1-mL portion of this HF solution was added to a green-brown solution of **1** (100 mg, 0.12 mmol) in 20 mL of CH_3CN. The color of the mixture changed immediately to a dark brown. This clear solution was allowed to evaporate slowly in the air. The dark crystalline solid that precipitated was collected by filtration, washed thoroughly with methanol, and finally dried in vacuum. This synthetic method provided a yield of 45 mg (46%). A single crystal for the X-ray structure determination (see below) was selected from this material. Anal. Calcd for $Mn_2C_{28}H_{34}N_6Cl_2F_2O_{10}$: Mn, 13.18; C, 40.36; H, 4.11; N, 10.08. Found: Mn, 13.0; C, 40.11; H, 3.98; N, 9.87. IR spectrum[12] (cm^{-1}): 1610(s), 1571(w), 1484(m), 1445(s), 1396(w), 1305(w), 1278(w), 1229(w), 1164(w), 1094(vs), 1053(sh), 1038(m), 1003(w), 848(w), 821(w), 798(m), 766(s), 719(w), 681(s), 666(w), 637(w), 622(s), 569(w), 526(m), 482(w), 438(w), 402(m). Electronic spectral data[12] in CH_3CN solution (λ_{max}, nm (ϵ, M^{-1} cm^{-1})): 780(144), 635(525), 530(660), 460(sh), 392(4800).

$[Mn_2O_2Cl_2(bpea)_2](ClO_4)_2$ (3). To an acetonitrile solution (10 mL) of 100 mg (0.12 mmol) of **1** was added 2 mL of 0.12 N HCl solution in CH_3CN. The HCl solution was prepared by diluting 0.1 mL of 12 N aqueous HCl to 10 mL by addition of CH_3CN. The green-brown color of the solution changed to brown immediately. This clear mixture was evaporated to dryness in the air at room temperature. The dark crystalline mass obtained was washed with CH_3OH and dried in vacuum. The isolated yield was 55 mg (54%). Anal. Calcd for $Mn_2C_{28}H_{34}N_6Cl_4O_{10}$: Mn, 12.68; Cl, 16.37; C, 38.82; H, 3.96; N, 9.70. Found: Mn, 12.4; Cl, 16.02; C, 38.59; H, 3.95; N, 9.55. IR spectrum[12] (cm^{-1}): 1607(s), 1571(w), 1481(s), 1463(w), 1443(s), 1396(w), 1302(m), 1281(s), 1252(w), 1229(w), 1144(m), 1091(vs), 1059(sh), 1035(m), 1018(w), 1000(w), 956(w), 898(w), 848(w), 821 (w), 798(m), 769(s), 716(w), 666(s), 657(m), 637(w), 625(s), 584(m), 564(w), 517(w), 482(w). Electronic spectral data[12] in CH_3CN solution (λ_{max}, nm (ϵ, M^{-1} cm^{-1})): 828(132), 642(580), 550(740), 450(sh), 420(sh), 380(sh).

X-ray Crystallography. $[Mn_2O_2(O_2CCH_3)(bpea)_2](ClO_4)_2$ (1). Single crystals were obtained by slow diffusion of hexane into a dichloromethane solution of **1** using the layering technique. A crystal of dimensions 0.25 × 0.41 × 0.60 mm was taken from the mother liquor, coated with oil (Paratone N, Exxon Chemical Co.), mounted on a glass fiber, and immediately transferred to an Enraf-Nonius CAD-4 diffractometer equipped with a low-temperature device which permitted the crystal to be bathed in a stream of dinitrogen at 180 K. Unit cell parameters were determined with use of a least-squares fitting routine using 24 reflections, including Friedel pairs, having 2θ values in the range 23−25°. The crystal stability was monitored by measuring the intensities of three check reflections every hour. No intensity reduction was observed in the 27.5 h of exposure to X-radiation. An absorption correction was applied to the data based on the ψ-scans[13] of four reflections with θ and χ values in the ranges 4−16 and 81−89°, respectively. The compound crystallizes as $1{\cdot}2CH_2Cl_2$ in the triclinic system. The structure was solved in the space group $P\bar{1}$ (No. 2) by direct methods[14] and refined by standard full-matrix least-squares and Fourier techniques on a Digital Equipment MicroVAX computer using locally modified Enraf-Nonius SDP software.[15] Significant crystal data are summarized in Table 1. All non-hydrogen atoms were refined using anisotropic thermal parameters. Hydrogen atoms of the ligands and CH_2Cl_2 molecules were located in a difference map and included in the structure factor calculation at idealized positions, but not refined. Atomic coordinates and equivalent isotropic thermal parameters for **1** are listed in Table 2.

Table 1. Crystallographic Data for $[Mn_2O_2(O_2CCH_3)(bpea)_2](ClO_4)_2{\cdot}2CH_2Cl_2$ ($1{\cdot}2CH_2Cl_2$), $[Mn_2O_2F_2(bpea)_2](ClO_4)_2$ (**2**), and $[Mn_2O_2Cl_2(bpea)_2](ClO_4)_2$ (**3**)

	$1{\cdot}2CH_2Cl_2$	**2**	**3**
chem formula	$Mn_2Cl_6O_{12}N_6C_{22}H_{41}$	$Mn_2Cl_2F_2O_{10}N_6C_{28}H_{34}$	$Mn_2Cl_4O_{10}N_6C_{28}H_{34}$
fw	1024.31	833.39	866.3
temp, K	180	130	128
space group	$P\bar{1}$	$P\bar{1}$	$P\bar{1}$
a, Å	9.293(2)	6.696(2)	7.187(2)
b, Å	12.233(2)	10.751(3)	10.669(3)
c, Å	18.812(3)	12.179(2)	12.531(3)
α, deg	92.781(13)	69.07(2)	113.72(2)
β, deg	99.636(19)	79.25(2)	99.73(2)
γ, deg	97.727(16)	81.46(3)	94.32(2)
V, Å^3	2083.6(15)	801.3(4)	856.0(4)
Z	2	1	1
d_{calcd}, g cm^{-3}	1.633	1.723	1.680
μ, cm^{-1}	10.33	86.47	94.36
λ, Å	0.710 73	1.541 78	1.541 78
R,[a] %	3.07	4.52	5.28
R_w,[b] %	3.92	4.50	5.63
GOF[c]	1.677	1.23	1.63

[a] $R = (\sum||F_o| - |F_c||)/\sum|F_o|$. [b] $R_w = \{[\sum w(|F_o| - |F_c|)^2]/\sum wF_o^2\}^{1/2}$. [c] $GOF = \{[\sum w(|F_o| - |F_c|)^2]/(n_o - n_v)\}^{1/2}$; $w = 4F_o^2/[\sigma(I)^2 + (pF_o^2)^2]$, where $p = 0.03$ (for $1{\cdot}2CH_2Cl_2$) and $w = (\sigma^2(F_o) + qF_o^2)^{-1}$, where $q = 0.0003$ (for **2**) and 0.001 (for **3**).

$[Mn_2O_2F_2(bpea)_2](ClO_4)_2$ (2). A crystal of dimensions 0.02 × 0.08 × 0.12 mm, grown as described above, was mounted in the cold stream (130 K) of a Siemens P4/RA diffractometer equipped with a LT-2 low-temperature apparatus. The radiation employed was Ni-filtered Cu Kα form a Siemens rotating-anode source operating at 15 kW. A mean fluctuation of 0.05% in the intensities of two reflections measured after every 198 reflections was observed during data collection. The structure was solved in the space group $P\bar{1}$ (No. 2) using a Patterson map and refined by full-matrix least-squares and different Fourier methods.[16] Selected crystal data are collected in Table 1. The asymmetric unit contains half of the molecule, as it resides on a crystallographic inversion center. A disordered methyl carbon in the ethyl group of bpea was refined with two sites having refined occupancies of 0.50(1) each. All non-hydrogen atoms were refined with anisotropic thermal parameters. Hydrogen atoms were added in calculated positions and refined by use of a riding model and fixed isotropic thermal parameters. Some of the hydrogen atoms of the disordered methyl carbons appeared on a difference map, and these were used to set the orientation of idealized methyl groups which were subsequently included in the structure factor calculation but not refined. An empirical correction for absorption based on F_o and F_c differences was applied by using the program XABS.[17] Atomic coordinates and equivalent isotropic thermal parameters are listed in Table 3.

$[Mn_2O_2Cl_2(bpea)_2](ClO_4)_2$ (3). Small single crystals were grown by allowing dichloromethane vapor to diffuse into an acetonitrile solution of **3**. A crystal of dimensions 0.02 × 0.04 × 0.08 mm was transferred to the cold stream (130 K) of a Siemens P4/RA diffractometer having a LT-2 low-temperature apparatus. A Siemens rotating-anode source operating at 15 kW provided the Ni-filtered Cu Kα

(12) Symbols: vs, very strong; s, strong; m, medium; w, weak; sh, shoulder.
(13) North, A. C. T.; Philips, D. C.; Mathews, F. S. *Acta Crystallogr., Sect. A* **1968**, *24*, 351−359.
(14) Sheldrick, G. M. SHELXS-86, A Program for X-ray Structure Determination; University of Gottingen: Gottingen, Germany, 1986.
(15) Frenz, B. A. Structure Determination Package; Texas A&M University and Enraf-Nonius: College Station, TX, and Dordrecht, The Netherlands, 1985 (as revised by Dr. F. J. Hollander).
(16) Sheldrick, G. M. SHELXTL PLUS, A Program for Crystal Structure Determination, Version 4.2; Siemens Analytical X-ray Instruments: Madison, WI, 1990.
(17) Hope, H.; Moezzi, B. XABS, Department of Chemistry, University of California, Davis.

Table 2. Atomic Coordinates and Equivalent Isotropic Thermal Parameters for $[Mn_2O_2(O_2CCH_3)(bpea)_2](ClO_4)_2{\cdot}2CH_2Cl_2$

atom	*x*	*y*	*z*	B,[a] Å^2
Mn1	0.10213(1)	0.22078(1)	0.19500(1)	1.39(1)
Mn2	0.02539(1)	0.41209(1)	0.23230(1)	1.49(1)
Cl1	0.3950(1)	0.74163(8)	0.03389(1)	2.73(2)
Cl2	0.3385(1)	0.82586(8)	0.55480(1)	2.91(2)
Cl3	0.1430(1)	0.20561(8)	0.54817(1)	3.71(2)
Cl4	0.4195(2)	0.3354(1)	0.61357(8)	6.52(4)
Cl5	0.1280(1)	0.2191(1)	0.76929(7)	5.59(3)
Cl6	0.3520(1)	0.08579(9)	0.74363(7)	4.48(3)
O1	−0.0650(2)	0.2688(2)	0.2061(1)	1.70(5)
O2	0.1967(2)	0.3474(2)	0.2425(1)	1.61(5)
O3	0.1165(2)	0.2774(2)	0.1016(1)	1.70(5)
O4	0.0438(2)	0.4429(2)	0.1204(1)	1.96(5)
O10	0.3751(4)	0.6628(3)	0.0859(2)	6.00(8)
O11	0.4089(4)	0.8485(3)	0.0683(2)	7.6(1)
O12	0.2710(4)	0.7240(3)	−0.0222(2)	6.07(9)
O13	0.5268(3)	0.7292(3)	0.0080(2)	5.85(8)
O20	0.1904(3)	0.7770(3)	0.5268(2)	4.69(8)
O21	0.4308(3)	0.7446(2)	0.5740(2)	4.78(8)
O22	0.3394(4)	0.8940(3)	0.6173(2)	8.8(1)
O23	0.3940(3)	0.8857(3)	0.5001(2)	5.87(8)
N1	0.2924(3)	0.1404(2)	0.1945(1)	1.63(6)
N2	0.1057(3)	0.1371(2)	0.2849(1)	1.62(6)
N3	0.0039(3)	0.0774(2)	0.1359(1)	1.65(6)
N4	−0.0091(3)	0.4449(2)	0.3495(1)	2.07(6)
N5	−0.1858(3)	0.4556(2)	0.2215(2)	2.14(6)
N6	0.1281(3)	0.5775(2)	0.2590(1)	1.62(6)
C1	0.3966(4)	0.1986(3)	0.1519(2)	2.16(8)
C2	0.5503(4)	0.1674(3)	0.1632(2)	3.26(9)
C3	0.3588(4)	0.1469(3)	0.2726(2)	1.96(7)
C4	0.2383(4)	0.1111(3)	0.3144(2)	1.69(7)
C5	0.2553(4)	0.0540(3)	0.3757(2)	2.01(7)
C6	0.1326(4)	0.0205(3)	0.4066(2)	2.25(8)
C7	−0.0024(4)	0.0468(3)	0.3759(2)	2.26(8)
C8	−0.0126(4)	0.1050(3)	0.3157(2)	1.84(7)
C9	0.2457(4)	0.0221(3)	0.1659(2)	1.99(7)
C10	0.0916(4)	0.0009(3)	0.1245(2)	1.71(7)
C11	0.0368(4)	−0.0923(3)	0.0788(2)	2.57(8)
C12	−0.1093(4)	−0.1084(3)	0.0461(2)	2.93(9)
C13	−0.1976(4)	−0.0301(3)	0.0588(2)	2.60(8)
C14	−0.1372(4)	0.0620(3)	0.1029(2)	2.12(7)
C15	0.0827(5)	0.3918(3)	0.4061(2)	3.05(9)
C16	0.2461(5)	0.4334(3)	0.4148(2)	3.7(1)
C17	−0.1661(4)	0.4008(3)	0.3446(2)	2.78(8)
C18	−0.2562(4)	0.4367(3)	0.2779(2)	2.50(8)
C19	−0.4036(4)	0.4491(3)	0.2719(2)	4.0(1)
C20	−0.4773(4)	0.4812(3)	0.2083(3)	4.4(1)
C21	−0.4056(4)	0.4983(3)	0.1516(2)	3.9(1)
C22	−0.2594(4)	0.4853(3)	0.1598(2)	2.85(9)
C23	0.0124(4)	0.5674(3)	0.3654(2)	2.48(8)
C24	0.1190(4)	0.6267(3)	0.3235(2)	1.80(7)
C25	0.1938(4)	0.7306(3)	0.3469(2)	2.46(8)
C26	0.2795(4)	0.7859(3)	0.3037(2)	2.73(8)
C27	0.2853(4)	0.7379(3)	0.2367(2)	2.46(8)
C28	0.2099(4)	0.6342(3)	0.2164(2)	2.02(7)
C29	0.0931(4)	0.3738(3)	0.0829(2)	2.04(7)
C30	0.1319(5)	0.4040(3)	0.0118(2)	3.38(9)
C31	0.3357(5)	0.2118(4)	0.5640(2)	4.2(1)
C32	0.3130(5)	0.2020(4)	0.7918(3)	4.6(1)

[a] The thermal parameter given for anisotropically refined atoms is the isotropic equivalent thermal parameter defined as $(4/3)[a^2B(1,1) + b^2B(2,2) + c^2B(3,3) + ab(\cos\gamma)B(1,2) + ac(\cos\beta)B(1,3) + bc(\cos\alpha)B(2,3)]$ where a, b, and c are real cell parameters and $B(i,j)$ are anisotropic β's.

radiation. A 1.3% decay in the intensities of two standard reflections measured after every 198 reflections was observed during data collection, and the data were scaled to correct for this effect. The structure was solved in the space group $P\bar{1}$ by using direct methods and refined by full-matrix least-squares and Fourier techniques.[16] Selected crystal data are summarized in Table 1. Due to the fact that the cation resides on a crystallographic inversion center, the asymmetric unit contains half of the dinuclear formula given above. The perchlorate anion is disordered into two alternative orientations; an equal occupancy for the two forms was assumed. One of the oxygen atoms (O2) is common to both forms. Mn and Cl atoms were refined with anisotropic thermal parameters. Hydrogen atoms were added geometrically and refined by using a riding model and fixed isotropic thermal parameters. Program XABS[17] was used for an absorption correction based on F_o and F_c differences. Atomic coordinates and equivalent isotropic thermal parameters for **3** are provided in Table 4.

Table 3. Atomic Coordinates ($\times 10^4$) and Equivalent Isotropic Displacement Coefficients (Å^2 $\times$ 10^3) for $[Mn_2O_2F_2(bpea)_2](ClO_4)_2$

atom[a]	*x*	*y*	*z*	U(eq)[b]
Mn	869(1)	3805(1)	690(1)	16(1)
O1	1506(5)	5128(3)	−685(3)	17(2)
F	3336(5)	2839(3)	574(3)	25(1)
N1	−376(7)	2481(4)	2314(4)	20(2)
N2	1874(7)	4510(4)	1791(4)	18(2)
N3	−340(7)	2592(5)	103(4)	19(2)
C1	895(9)	4096(6)	2927(5)	18(2)
C2	1515(10)	4435(6)	3786(5)	24(3)
C3	3149(9)	5212(6)	3490(5)	27(3)
C4	4111(9)	5620(6)	2337(5)	21(3)
C5	3465(8)	5242(6)	1499(5)	18(2)
C6	−860(9)	3282(6)	3123(5)	22(2)
C7	−2258(9)	2114(6)	2062(5)	25(3)
C8	−1814(9)	1870(6)	899(5)	19(2)
C9	−2799(9)	1022(6)	608(5)	22(3)
C10	−2294(9)	933(6)	−523(5)	23(3)
C11	−770(9)	1648(6)	−1319(5)	23(3)
C12	192(9)	2472(5)	−978(5)	21(3)
C13	1034(11)	1244(6)	2781(5)	38(3)
C14a	2648(19)	1272(12)	3236(11)	27(6)
C14b	722(19)	453(12)	4034(11)	29(6)
Cl	4050(2)	2135(2)	6296(1)	30(1)
O2	5159(7)	1530(5)	7288(4)	48(2)
O3	5451(7)	2472(5)	5213(4)	45(2)
O4	2870(6)	3338(4)	639(3)	33(2)
O5	2693(7)	1223(5)	6287(4)	48(2)

[a] Equivalent isotropic U defined as one-third of the trace of the orthogonalized U_{ij} tensor.

Results and Discussion

Synthesis and Solution Characteristics. Preparation of the mixed-valence complex $[Mn_2O_2(O_2CCH_3)(bpea)_2](ClO_4)_2$ (**1**) was carried out by using a procedure that employs manganese(II) acetate and permanganate as oxidant, as established for the well-known bipyridyl-ligated species $[Mn_2O_2(bpy)_4](ClO_4)_3$.[18] In our hands, the other oxidants commonly used in the preparation of bis(μ-oxo) $Mn^{III}Mn^{IV}$ complexes such as (i) dioxygen,[19] (ii) H_2O_2,[20] and (iii) disproportionative oxidation of Mn(III) precursors[7,21,22] were unsuccessful. Complex **1** is soluble in CH_2Cl_2, CH_3CN, and $(CH_3)_2CO$, giving a green-brown solution. In solution, complex **1** is remarkably less stable

(18) Cooper, S. R.; Calvin, M. *J. Am. Chem. Soc.* **1977**, *99*, 6623−6630.
(19) (a) Brewer, K. J.; Calvin, M.; Lumpkin, R. S.; Otvos, J. W.; Spreer, L. O. *Inorg. Chem.* **1989**, *28*, 4446−4451. (b) Hagen, K. S.; Armstrong, W. H.; Hope, H. *Inorg. Chem.* **1988**, *27*, 967−969. (c) Goodson, P. A.; Hodgson, D. J.; Glerup, J.; Michelsen, K.; Weihe, H. *Inorg. Chim. Acta* **1992**, *197*, 141−147.
(20) (a) Goodson, P. A.; Glerup, J.; Hodgson, D. J.; Michelsen, K.; Weihe, H. *Inorg. Chem.* **1991**, *30*, 4909−4914. (b) Oki, A. R.; Glerup, J.; Hodgson, D. J. *Inorg. Chem.* **1990**, *29*, 2435−2441. (c) Goodson, P. A.; Glerup, J.; Hodgson, D. J.; Michelsen, K.; Pedersen, E. *Inorg. Chem.* **1990**, *29*, 503−508. (d) Goodson, P. A.; Hodgson, D. J.; Michelsen, K. *Inorg. Chim. Acta* **1990**, *172*, 49−57. (e) Towle, D. K.; Botsford, C. A.; Hodgson, D. J. *Inorg. Chim. Acta* **1988**, *141*, 167−168. (f) Suzuki, M.; Senda, H.; Kobayashi, Y.; Oshio, O.; Uehara, A. *Chem. Lett.* **1988**, 1763−1766. (g) Collins, M. A.; Hodgson, D. J.; Michelsen, K.; Pedersen, E. *J. Chem. Soc., Chem. Commun.* **1987**, 1659−1660.
(21) (a) Stebler, M.; Ludi, A.; Bürgi, H.-B. *Inorg. Chem.* **1986**, *25*, 4743−4750. (b) Usón, R.; Riera, V.; Ciriano, M. A. *Transition Met. Chem. (London)* **1976**, *1*, 98−99. (c) Plaksin, P. M.; Stoufer, R. C.; Matthew, M.; Palenik, G. J. *J. Am. Chem. Soc.* **1972**, *94*, 2121−2122.

Table 4. Atomic Coordinates ($\times 10^4$ and Equivalent Isotropic Displacement Coefficients ($Å^2 \times 10^3$) for $[Mn_2O_2Cl_2(bpea)_2](ClO_4)_2$

atom	*x*	*y*	*z*	*U*(eq)[a]
Mn	598(2)	5581(1)	4288(1)	14(1)
Cl1	3407(2)	6837(2)	4438(2)	20(1)
O1	1504(7)	5422(5)	5657(4)	19(1)
N1	−971(8)	5517(6)	2696(5)	16(1)
N2	1376(8)	3897(6)	3111(5)	16(1)
N3	−446(8)	7362(6)	4959(5)	15(1)
C1	216(10)	3320(7)	2023(7)	19(2)
C2	629(11)	2169(8)	1100(7)	26(2)
C3	2250(11)	1652(9)	1332(8)	28(2)
C4	3451(11)	2245(8)	2462(7)	23(2)
C5	2978(10)	3377(8)	3328(7)	20(2)
C6	−1518(10)	3990(7)	1890(7)	21(2)
C7	−2634(10)	6203(8)	3039(7)	21(2)
C8	−1939(10)	7471(7)	4197(6)	15(2)
C9	−2746(10)	8674(7)	4523(7)	18(2)
C10	−2040(11)	9726(8)	5649(7)	24(2)
C11	−487(11)	9602(8)	6397(7)	23(2)
C12	290(11)	8417(8)	6029(7)	19(2)
C13	129(10)	6236(8)	2126(7)	20(2)
C14	−1005(12)	6301(9)	1020(8)	31(2)
Cl2	4409(3)	8373(2)	1260(2)	31(1)
O2	4309(9)	6921(6)	985(6)	52(2)
O3a	4599(20)	8548(13)	199(9)	56(6)
O4a	5901(15)	9198(10)	2243(9)	45(4)
O5a	2583(13)	8782(10)	1525(11)	36(3)
O3b	3964(20)	8589(12)	192(9)	34(4)
O4b	6363(16)	9067(13)	1869(13)	56(4)
O5b	3103(21)	8940(14)	1997(13)	67(5)

[a] The atoms labeled a and b are parts of a disordered (50:50) perchlorate group. [b] Equivalent isotropic *U* defined as one-third of the trace of the orthogonalized U_{ij} tensor.

than the tpen analog $[Mn_2O_2(O_2CCH_3)(tpen)]^{2+}$.[22a] For example, addition of small quantities of water to a CH_3CN solution of **1** results in the immediate precipitation of an insoluble brown material whereas the characteristic green color of the tpen analog in pure water persists for a much longer period of time. Also, high-return recrystallization of the tpen analog is possible under ambient conditions whereas if the same is attempted for compound **1**, extensive loss of starting material due to decomposition is observed. We postulate that the observed instability of **1** is due to a pronounced lability of the Mn(III) center caused by the severe distortion of the $Mn^{III}N_3O_3$ coordination sphere as determined by X-ray crystallography (vide infra). The issue of the instability of **1** is of interest to us in connection with our goal of achieving controlled formation of a dimer of dimers within this ligand system. The formation of $[Mn_2O_2X_2(bpea)_2](ClO_4)_2$ (X = F, **2**; X = Cl, **3**) by the addition of HX to an acetonitrile solution of **1** is likely accompanied by generation of a lower valent product in a disproportionation reaction. The yields of **2** and **3**, ~50% with respect to total manganese, support the hypothesis of a disproportionative process in which half of the starting material is converted to the herein characterized IV,-IV dimers, while the remaining manganese ends up in the +3 oxidation state. The nature of the lower oxidation state product or products is currently under investigation. Evidence for disproportionation of binuclear $Mn^{III}Mn^{IV}$ complexes under acidic conditions has been noted previously.[5,18,23] Also, it should

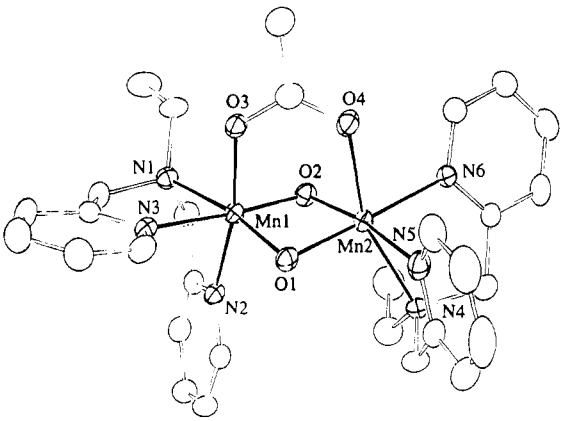

Figure 1. Structure of $[Mn_2O_2(O_2CCH_3)(bpea)_2]^{2+}$ (**1**) showing 50% probability thermal ellipsoids. For clarity, hydrogen atoms are omitted and carbon atoms are not labeled.

be noted that the generation of compounds similar to **2** and **3**, namely $[Mn_2O_2X_2(tacn)_2]^{2+}$ (X = F, Cl), in aqueous acid from a $Mn^{III}Mn^{IV}$ precursor has been explained[7] to be the result of a disproportionation process.

Description of Structures. $[Mn_2O_2(O_2CCH_3)(bpea)_2](ClO_4)_2$ (1). The crystal structure of **1** is shown in Figure 1. The tripodal ligand bpea binds each Mn atom in a facial configuration. The other three coordination sites of both the Mn atoms are occupied by the two μ-oxo atoms and the oxygen atoms of the bridging acetate group. The Mn(IV) and Mn(III) ions (Mn1 and Mn2, respectively) are clearly distinguishable in **1** on the basis of bond distances (Table 5). The Mn···Mn distance (2.6333(7) Å) is within the range (2.588(2)−2.741(1) Å) observed for other structurally characterized $Mn^{III}Mn^{IV}$ dioxo-bridged complexes[7,19,20,21a,c,23] but is slightly longer than that (2.580(1) Å) of the corresponding $Mn^{IV}Mn^{IV}$ analog.[5] An interesting feature in the structure of **1** is its asymmetry as evidenced in the different binding modes adopted by bpea for the Mn(III) and Mn(IV) centers. The aliphatic nitrogen atom (N4) is *trans* to the acetate oxygen atom (O4) at the Mn(III) center, whereas the corresponding atoms (N1 and O3) are oriented *cis* to each other at the Mn(IV) center. In the Mn^{IV}-Mn^{IV} analogue[5] of **1**, bpea binds both Mn(IV) ions in the same manner as it does the Mn(IV) ion in **1**. The $Mn^{III}N_3O_3$ octahedron in **1** is very distorted (Figure 1, Table 5), in part owing to Jahn−Teller elongation along the axis N4−Mn2−O4. The Mn2−N4 bond distance (2.305(3) Å) is substantially longer than any other Mn−N distance in the cation. The distortion is also manifested in a N4−Mn2−O4 angle (159.25-(9)°) that deviates significantly from linearity. We propose that an important factor in the above mentioned instability of **1** is this distortion at the Mn(III) center. Attack at the Mn(III) center by water or hydroxide may be facilitated by the opening of the N4−Mn2−O4 angle (see Figure 1). As in other compounds containing the $\{Mn_2O_2(O_2CCH_3)\}^{2+/3+}$ core,[5,22,23a] the four-membered $\{Mn_2(\mu\text{-}O)_2\}$ ring in **1** is not planar. The dihedral angle between the best least-squares planes containing atoms Mn1,O1,O2 and Mn2,O1,O2 is 160.7(2)°. This dihedral angle is significantly smaller than that in the corresponding Mn^{IV}-Mn^{IV} analog (164.7(3)°).[5]

$[Mn_2O_2F_2(bpea)_2](ClO_4)_2$ (2). This is the first structurally characterized compound containing an $\{Mn_2O_2\}$ core with terminally coordinated fluoride ions. The cation resides on a crystallographic inversion center (Figure 2). Each Mn atom is coordinated by three nitrogen atoms of bpea, one fluoride ion, and two μ-oxo oxygen atoms. An unexpected feature of the structure is the meridional binding mode of bpea as compared to the facial coordination mode observed for the synthetic

(22) (a) Pal, S.; Gohdes, J. W.; Wilisch, W. C. A.; Armstrong, W. H. *Inorg. Chem.* **1992**, *31*, 713−716. (b) Bashkin, J. S.; Schake, A. R.; Vincent, J. B.; Chang, H.-R.; Li, Q.; Huffman, J. C.; Christou, G.; Hendrickson, D. N. *J. Chem. Soc., Chem. Commun.* **1988**, 700−702. (c) Mahapatra, S.; Das, P.; Mukherjee, R. *J. Chem. Soc., Dalton Trans.* **1993**, 217−220.

(23) (a) Pal, S.; Armstrong, W. H. *Inorg. Chem.* **1992**, *31*, 5417−5423. (b) Sarneski, J. E.; Didiuk, M.; Thorp, H. H.; Crabtree, R. H.; Brudvig, G. W.; Faller, J. W.; Chulte, G. K. *Inorg. Chem.* **1991**, *30*, 2833−2835.

Table 5. Selected Bond Distances and Angles for $[Mn_2O_2(O_2CCH_3)(bpea)_2](ClO_4)_2 \cdot 2CH_2Cl_2$[a]

			Distances (Å)		
Mn1–O1	1.772(2)	Mn1–N2	2.017(3)	Mn2–O4	2.187(2)
Mn1–O2	1.791(2)	Mn1–N3	2.046(3)	Mn2–N4	2.305(3)
Mn1–O3	1.938(2)	Mn2–O1	1.845(2)	Mn2–N5	2.082(3)
Mn1–N1	2.137(3)	Mn2–O2	1.857(2)	Mn2–N6	2.117(3)
			Angles (deg)		
O1–Mn1–O2	87.4(1)	O3–Mn1–N2	168.7(1)	O2–Mn2–O4	90.33(9)
O1–Mn1–O3	97.6(1)	O3–Mn1–N3	84.6(1)	O2–Mn2–N4	103.8(1)
O1–Mn1–N1	169.5(1)	N1–Mn1–N2	78.3(1)	O2–Mn2–N5	169.6(1)
O1–Mn1–N2	91.9(1)	N1–Mn1–N3	80.9(1)	O2–Mn2–N6	97.0(1)
O1–Mn1–N3	95.5(1)	N2–Mn1–N3	88.3(1)	O4–Mn2–N4	159.25(9)
O2–Mn1–O3	92.5(1)	O1–Mn2–O2	83.33(9)	O4–Mn2–N5	93.1(1)
O2–Mn1–N1	96.7(1)	O1–Mn2–O4	91.93(9)	O4–Mn2–N6	86.34(9)
O2–Mn1–N2	94.2(1)	O1–Mn2–N4	104.6(1)	N4–Mn2–N5	75.7(1)
O2–Mn1–N3	176.1(1)	O1–Mn2–N5	86.8(1)	N4–Mn2–N6	77.0(1)
O3–Mn1–N1	91.9(1)	O1–Mn2–N6	178.2(1)	N5–Mn2–N6	93.0(1)
Mn1–O2–Mn2	92.4(1)	Mn1–O1–Mn2	93.4(1)		

[a] Numbers in parentheses are estimated standard deviations in the least significant digits.

Table 6. Selected Bond Distances and Angles for $[Mn_2O_2F_2(bpea)_2](ClO_4)_2$[a]

			Distances (Å)		
Mn–O1	1.795(3)	Mn–F	1.827(3)	Mn–N2	2.010(6)
Mn–O1′	1.817(4)	Mn–N1	2.088(4)	Mn–N3	2.015(6)
			Angles (deg)		
O1–Mn–O1′	81.0(2)	O1′–Mn–F	175.1(1)	N1–Mn–N2	80.8(2)
O1–Mn–F	94.0(1)	O1′–Mn–N1	88.4(2)	N1–Mn–N3	80.4(2)
O1–Mn–N1	169.5(2)	O1′–Mn–N2	91.9(2)	N2–Mn–F	88.8(2)
O1–Mn–N2	99.0(2)	O1′–Mn–N3	91.8(2)	N2–Mn–N3	160.7(2)
O1–Mn–N3	100.3(2)	N1–Mn–F	96.5(2)	N3–Mn–F	89.1(2)
Mn–O1–Mn′	99.0(2)				

[a] Numbers in parentheses are estimated standard deviations in the least significant digits.

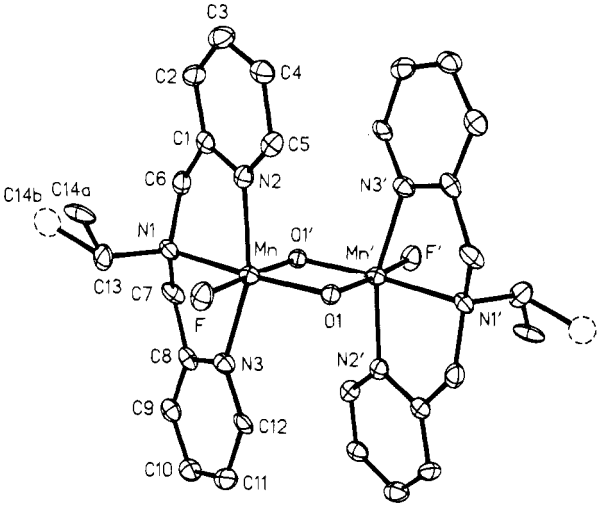

Figure 2. Structure of $[Mn_2O_2F_2(bpea)_2]^{2+}$ (**2**) with the atom-labeling scheme. All atoms are represents by their 50% probability thermal ellipsoids. Hydrogen atoms are omitted for clarity.

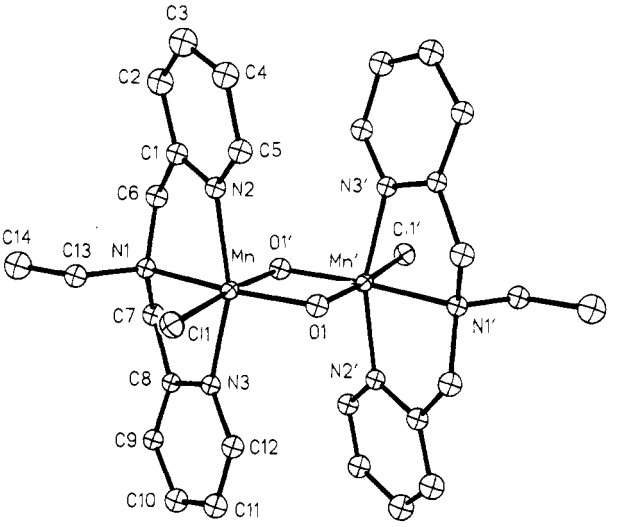

Figure 3. Structure of $[Mn_2O_2Cl_2(bpea)_2]^{2+}$ (**3**) showing 50% probability thermal ellipsoids and the atom-labeling scheme. Hydrogen atoms are omitted for clarity.

precursor (**1**). The longer Mn–O1′ distance (1.817(4) Å) compared to the Mn–O1 bond length (1.795(3) Å) is indicative that fluoride ion has a greater *trans* influence than the tertiary nitrogen atom in bpea. The Mn–F bond distance (1.827(3) Å) in **2** is larger compared to terminal Mn–F distances observed in two other structurally characterized complexes: $[Mn_2F_9]^-$ (terminal Mn–F, 1.71 Å; bridging Mn–F, 1.89 Å)[24] and $[MnF_6]^{2-}$ (Mn–F, 1.79 Å).[25] The Mn···Mn distance (2.746(2) Å) is on the high end of the range (2.580(1)–2.748(2) Å) observed for structurally characterized $Mn^{IV}_2O_2$ complexes prior to this work.[5,20a–c,21a,23,26] The remaining bond distances and angles at the Mn(IV) center are unexceptional. Selected bonding parameters are collected in Table 6.

$[Mn_2O_2Cl_2(bpea)_2](ClO_4)_2$ (3). The structure of **3** (Figure 3) is very similar to that of the fluoro analog (**2**). In contrast to the situation for **2** however, Mn–O_{oxo} distances *cis* and *trans* to the chloride ligand are virtually identical within experimental error: Mn–O1 (1.809(6) Å) and Mn–O1′ (1.812(5) Å). There are two other examples of complexes which contain the $\{Mn_2(\mu$-

(24) Muller, B. G. *J. Fluorine Chem.* **1981**, *17*, 409–421.
(25) Bukovec, P.; Hoppe, R. *J. Fluorine Chem.* **1983**, *23*, 579–587.
(26) (a) Larson, E.; Lah, M. S.; Li, X.; Bonadies, J. A.; Pecoraro, V. L. *Inorg. Chem.* **1992**, *31*, 373–378. (b) Gohdes, J. W.; Armstrong, W. H. *Inorg. Chem.* **1992**, *31*, 368–373. (c) Libby, E.; Webb, R. J.; Streib, W. E.; Folting, K.; Huffman, J. C.; Hendrickson, D. N.; Christou, G. *Inorg. Chem.* **1989**, *28*, 4037–4040.

Table 7. Selected Bond Distances and Angles for $[Mn_2O_2Cl_2(bpea)_2](ClO_4)_2$[a]

		Distances (Å)			
Mn−O1	1.809(6)	Mn−Cl1	2.273(2)	Mn−N2	2.003(6)
Mn−O1′	1.812(5)	Mn−N1	2.091(7)	Mn−N3	2.006(6)
		Angles (deg)			
O1−Mn−O1′	80.8(2)	O1′−Mn−Cl1	172.9(2)	N1−Mn−N2	80.3(2)
O1−Mn−Cl1	92.0(2)	O1′−Mn−N1	87.2(3)	N1−Mn−N3	81.1(2)
O1−Mn−N1	168.0(3)	O1′−Mn−N2	92.4(2)	N2−Mn−Cl1	89.0(2)
O1−Mn−N2	99.9(3)	O1′−Mn−N3	92.4(2)	N2−Mn−N3	160.5(3)
O1−Mn−N3	99.5(2)	N1−Mn−Cl1	100.0(2)	N3−Mn−Cl1	88.5(2)
Mn−O1−Mn′	99.2(2)				

[a] Numbers in parentheses are estimated standard deviations in the least significant digits.

$O)_2Cl_2\}$ unit with chloride ligands bound in the Mn_2O_2 plane: (i) a mixed-valence (III,IV) complex, $[Mn_2O_2Cl_2(O_2CCH_3)(bpy)_2]$,[22b] and (ii) $[Mn_3O_4Cl_2(bpy)_4]^{2+}$.[27] In both cases, elongation of Mn−O bonds *trans* to the coordinated chloride atoms is evident. The Mn−Cl bond length (2.273(2) Å) in **3** is shorter than the Mn(IV)−Cl distances observed for the above two complexes: (i) 2.3414(26) Å and (ii) 2.336(5) Å. The Mn···Mn distance in **3** (2.757(3) Å) is the largest one among all the structurally characterized $\{Mn^{IV}_2O_2\}$ complexes.[5,20a−c,21a,23,26] Selected bond distances and angles for **3** are listed in Table 7.

Physical Properties. As for other complexes[5,22,23a] containing the $\{Mn_2O_2(O_2CCH_3)\}$ core, the infrared spectrum of compound **1** displays prominent ν_{as} (1563 cm^{-1}) and ν_s (1387 cm^{-1}) vibrations of the O−C−O portion of the μ-acetate group. In addition to bpea-related signals, complex **1** shows an intense peak at 693 cm^{-1}. Resonances in the range 669−694 cm^{-1} found for related complexes[5,18,19,22a,23a,28] have been assigned to the breathing mode of the $\{Mn_2O_2\}$ core.[28] IR spectra of representative bulk samples of both **2** and **3** lack the μ-acetate stretches, indicating the absence of starting material. As for **1**, sharp and intense resonances at 681 cm^{-1} for **2** and 666 cm^{-1} for **3** are presumably associated with the breathing mode of the $\{Mn_2O_2\}^{4+}$ core unit.[28]

The electronic spectrum of complex **1** in acetonitrile (not shown) displays the characteristic pattern of an $\{Mn_2O_2\}^{3+}$ core.[18,19,20,22] Maxima are observed at 633 nm (ϵ = 350 M^{-1} cm^{-1}) and 545 nm (ϵ = 420 M^{-1} cm^{-1}). While these peak positions are similar to those found for compounds with the planar $\{Mn_2O_2\}^{3+}$ core, the intensities are significantly smaller on average. Recently, this decrease in intensity for bands in the visible region was correlated with bending of the Mn_2O_2 core.[29] In addition to the aforementioned maxima, shoulders at 490 and 455 nm are displayed for **1**. Several authors[18,19a,20c] have speculated about assignments for the absorption bands in the visible region of compounds that contain the $\{Mn_2(\mu\text{-}O)_2\}^{3+/4+}$ core. There appears to be a growing consensus that the absorption in the vicinity of 650 nm is oxo-to-Mn(IV) charge transfer in origin, while that at approximately 550 nm corresponds to a d−d band. Further supporting evidence for these and other assignments, based on magnetic circular dichroism measurements for **1** and other species, was reported elsewhere.[29] An absorption at 830 nm for $[Mn_2O_2(bpy)_4]^{3+}$ was previously assigned[18] as an intervalence transition. It was estimated recently that the intervalence band should occur at approximately 998 nm on the basis of an ab initio calculation done in conjunction with X-ray scattering measurements.[30] The tpen analog of **1**, $[Mn_2O_2(O_2CCH_3)(tpen)]^{2+}$,[22a] shows a distinct absorption at 855 nm. On the other hand, no such putative intervalence transition has been observed for **1**. The peak at 633 nm has a broad tail to lower energy, and it is possible that another transition is underlying it. A similar observation was made for $[Mn_2O_2(cyclam)_2]^{3+}$.[19a] As for the bpy complex mentioned above, the low-energy tail for the cyclam species was attributed to an intervalance transistion. The evidence supporting this assignment is not compelling, especially considering the recent MCD study by Solomon and co-workers.[29]

In terms of the numbers of bands and their approximate positions, the electronic spectra of **2** and **3** (not shown) are similar. In the visible region, compound **2** displays absorption maxima at 635 nm (ϵ = 525 M^{-1} cm^{-1}) and 530 nm (ϵ = 660 M^{-1} cm^{-1}). For complex **3**, the band positions (at 645 nm, ϵ = 660 M^{-1} cm^{-1}, and 549 nm, ϵ = 821 M^{-1} cm^{-1}) are shifted to slightly lower energy. Assuming that the lower energy band is an oxo-to-metal charge transfer transition (see above), the shift to lower energy for the chloride relative to the fluoride dimer is consistent with a lowering of the relevant d orbital energy for **3** in relation to **2**. This is consistent with the observation that **3** is easier to reduce electrochemically than **2** (see below). A yet lower energy band is observed for both **2** (780 nm, ϵ = 144 M^{-1} cm^{-1}) and **3** (828 nm, ϵ = 132 M^{-1} cm^{-1}). Absorptions in the vicinity of 800 nm were reported previously for $\{Mn^{IV}_2O_2\}^{4+}$ complexes.[5,19c,20a,c,23a,31] The origin of this low-energy band is not understood at present. It is interesting to note that, as mentioned above, features at similar energies in absorption spectra of mixed-valence (III,IV) complexes have been assigned to intervalence transitions.

In frozen (77 K) acetonitrile−toluene (1:1) solution, complex **1** displays an EPR signal (not shown) centered at g = 2.05 with 16 nuclear hyperfine lines, a pattern commonly observed for species with the dioxo-bridged dimanganese(III,IV) core. This signal originates from the cation's $S = {}^1/_2$ ground state, which is the level predominantly populated at liquid nitrogen temperature, as borne out by magnetic susceptibility data (see below). The average ^{55}Mn hyperfine splitting for **1** is 86 G. In contrast to the situation for the the tpen analog,[22a] no anisotropy is observed in the EPR spectrum of compound **1**. As anticipated, since they have S = 0 ground states and even-spin excited states, complexes **2** and **3** do not display prominent EPR signals at 77K.[33]

The cyclic voltammogram of **1** in acetonitrile, shown in Figure 4, displays one quasi-reversible oxidation wave at $E_{1/2}$ = +0.92 V (ΔE_p = 80 mV)[32] and one reduction wave at $E_{1/2}$

(27) Auger, N.; Girerd, J.-J.; Corbella, M.; Gleizes, A.; Zimmermann, J.-L. *J. Am. Chem. Soc.* **1990**, *112*, 448−450.
(28) Czernuszewicz, R. S.; Dave, B.; Rankin, J. G. In *Spectroscopy of Biological Molecules*; Hester, R. E., Girling, R. B., Eds.; Royal Chemical Society Press: Cambridge, U. K., 1991; pp 285−288.
(29) Gamelin, D. R.; Kirk, M. L.; Stemmler, T. L.; Pal, S.; Armstrong, W. H.; Penner-Hahn, J. E.; Solomon, E. I. *J. Am. Chem. Soc.* **1994**, *116*, 2392.
(30) Gao, Y.; Frost-Jensen, A.; Pressprich, M. R.; Coppens, P.; Marquez, A.; Dupuis, M. *J. Am. Chem. Soc.* **1992**, *114*, 9214−9215.
(31) Gohdes, J. W. Ph.D. Dissertation, University of California, Berkeley, 1991.
(32) Abbreviations: E_{pa}, anodic peak potentia; E_{pc}, cathodic peak potential; $E_{1/2} = (E_{pa} + E_{pc})/2$; $\Delta E_p = E_{pa} - E_{pc}$.

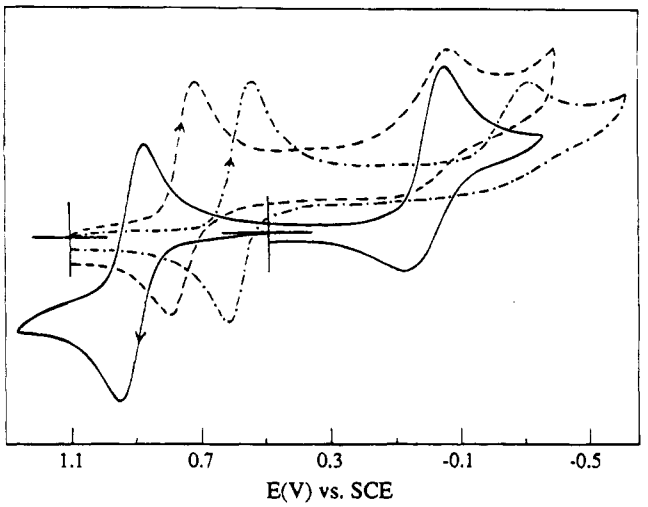

Figure 4. Cyclic voltammograms of **1** (—), **2** (— • — •), and **3** (- - -) in CH_3CN (0.1 M TEAP for **1** and **3**; 0.1 M *n*-Bu_4NPF_6 for **2** at a platinum electrode (scan rate 50 mV s^{-1}).

= +0.02 V (ΔE_p = 120 mV) vs SCE corresponding to the III,-IV/IV,IV and III,III/III,IV couples, respectively. The positions of the above couples for the isolated $Mn^{IV}Mn^{IV}$ analog of **1** were previously determined to be at +0.93 and +0.03 V vs SCE.[5] Thus, although the binding mode of bpea at the Mn(III) center in **1** is different from that of the Mn(IV) centers in **1** and its IV,IV analog, apparently there is no dramatic effect on the potential of the III,IV/IV,IV couple. Both complexes **2** and **3** display quasi-reversible IV,IV/IV,III and irreversible III,IV/III,-III reduction responses (Figure 4) in acetonitrile. The potentials for these two reductions are $E_{1/2}$ = +0.59 V (ΔE_p = 80 mV), E_{pc} = −0.35 V for **2** and $E_{1/2}$ = +0.74 V (ΔE_p = 80 mV), E_{pc} = −0.06 V for **3**. The more negative potentials for **2** compared to **3** are consistent with the stronger basicity of F^- compared to Cl^-. A comparable shift in the reduction potential of MnPSII may explain why water oxidation is inhibited when chloride is replaced by fluoride therein. At this time, no comparison among **2**, **3**, and their tacn analogs can be made, as the electrochemical properties of the last were not reported.[7]

Magnetic susceptibility measurements on a powdered sample of **1** were conducted in the temperature range 6−280 K at a constant applied magnetic field of 5 kG. The effective magnetic moment (μ_{eff}) of **1** at 6 K (1.84 μ_B) is in good agreement with the calculated spin-only moment for a single unpaired electron (1.73 μ_B). The moment changes very little up to 120 K (1.87 μ_B) and then gradually increases to 2.24 μ_B at 280 K. The data were fit by using an expression for χ_M vs T obtained from the isotropic spin-exchange Hamiltonian[34] $\mathcal{H} = -2JS_1 \cdot S_2$, where $S_1 = 2$ (for the Mn(III) ion) and $S_2 = {}^3/_2$ (for the Mn(IV) ion). A satisfactory fit was obtained by least-squares refinement with $J = -164$ cm^{-1}, $g = 2.0$ (fixed), and $P = 1.1$, where P is the mole percent of a paramagnetic impurity assumed to be a Mn-(III) monomer. This value of J is substantially larger than that of the corresponding tpen analog $[Mn_2O_2(O_2CCH_3)(tpen)]^{2+}$ (−125 cm^{-1})[22a] and $[Mn_2O_2Cl_2(O_2CCH_3)(bpy)_2]$ (−114 cm^{-1})[22b] but smaller than the coupling constant reported for the tacn compound[7] $[Mn_2O_2(O_2CCH_3)(tacn)_2]^{2+}$ (−220 cm^{-1}). A reasonably wide range (−114 to −272 cm^{-1}) of J values has been observed for complexes[19b,c,20a−d,f,21a,35] with the $\{Mn_2O_2\}^{3+}$ core. To date, a satisfactory magneto−structural correlation for this class of compounds has not appeared in the literature.

One of the novel dihalide dimanganese(IV) species, namely **3**, was also characterized by variable susceptibility measurements. As for **1**, data were collected in the range 6−280 K using an applied magnetic field strength of 5 kG. Using the expression derived from the standard isotropic spin-exchange Hamiltonian as above, but in this case with two $S = {}^3/_2$ ions, a suitable fit was obtained with g fixed at 2.0 using the following variable parameters: $J = -147$ cm^{-1}, $P = 0.99\%$, and TIP = 2.54×10^{-3}, where TIP is the temperature-independent paramagnetism. This value for J is within the range observed for complexes with the dioxo-bridged dimanganese(IV) core; thus a chloro ligand in the Mn_2O_2 plane does not have a dramatic effect on the Mn···Mn magnetic coupling.

In conclusion, a novel binuclear trapped valence complex of the tripodal ligand bpea having the $\{Mn_2O_2(O_2CCH_3)\}^{2+}$ core (**1**) has been prepared. This represents a rare example of an asymmetric dioxodimanganese(III,IV) core.[36] Here, the asymmetry is a result of different binding modes adopted by bpea at the Mn(III) versus the Mn(IV) site. The bulk spectral, electrochemical, and magnetic properties of **1** are as expected for a species with the $\{Mn_2O_2\}^{3+}$ unit. The acetate bridge in **1** can be replaced with two fluoride or two chloride ligands using aqueous HF or HCl, respectively. Yields of the halide-ligated products **2** and **3** are consistent with a disproportionative process where half of the manganese in the III,IV starting material is recovered in the IV,IV oxidation level and the other half presumably goes to the Mn(III) level. It is interesting to note that the tridentate ligand bpea adopts the facial coordination mode in **1** but instead the meridional mode in both **2** and **3**. Thus bpea is distinctly more flexible in this regard relative to ligands such as tacn or hydrotris(1-pyrazolyl)borate. Currently, in connection with our goal of achieving an accurate structural model for MnPSII, we are attempting to initiate controlled aggregative processes using the halide dimers. Also, we anticipate that compound **1** itself may be a useful starting material for tetramer formation owing to its observed remarkable lability, which we ascribed at least in part to the pronounced distortion in its Mn(III) coordination sphere.

Acknowledgment. Funding for this work was provided by National Institutes of Health Grant GM38275. W.H.A. is grateful for a Presidential Young Investigator Award from the national Science Foundation (1988−1993, CHE-8857455). The W. M. Feck Foundation provided funds for the SQUID magnetometer at Tufts University.

Supporting Information Available: A fully labeled ORTEP drawing of **1**, tables of complete crystallographic data, hydrogen positional and isotropic thermal parameters, anisotropic thermal parameters, intramolecular bond distances, and intramolecular bond angles for **1**−**3**, and a table of experimental and calculated molar susceptibilities as a function of temperature for **1** and **3** (12 pages). Ordering information is given on any current masthead page.

IC930020K

(33) Dexheimer, S. L.; Gohdes, J. W.; Chan, M. K.; Hagen, K. S.; Armstrong, W. H.; Klein, M. P. *J. Am. Chem. Soc.* **1989**, *111*, 8923−8925.
(34) O'Connor, C. J. *Prog. Inorg. Chem.* **1982**, *29*, 204−283.
(35) Cooper, S. R.; Dismukes, G. C.; Klein, M. P.; Calvin, M. *J. Am. Chem. Soc.* **1978**, *100*, 7248−7252.
(36) For another recent example, see: Bossek, U.; Saher, M.; Weyhermüller, T.; Wieghardt, K. *J. Chem. Soc., Chem. Commun.* **1992**, 1780−1782.